# Appendix C

Vanadium Oxo and Oxomethoxo Cluster Anions with Electro-Spray

Vanadium oxide cluster anions discussed in Chapter 3 are always found to have the predicted most stable structures. Cluster anions are produced by laser vaporization, i.e., progressively built up from atomic components present in the laser generated plasma. An interesting question is whether it is possible to generate different isomers, for example by producing the clusters with a different technique. This is of major relevance since it can deliver a recipe for controlling the production of different isomers in a controlled manner. Moreover, these experiments can help the understanding of the microscopical mechanisms involved in the cluster production in different ion sources. In this appendix, a different approach for the production of gas phase vanadium oxide and vanadium oxide methoxo cluster anions is explored, namely electrospray ionization. A milli-molar solution of $V_6O_7(OCH_3)_{12}$ [297] in methanol is sprayed with a flow rate of $\sim$2 μL/min. Several fragments of the precursor are obtained by spraying under relatively harsh electrospray ionization conditions. Fragment clusters with the general formula $V_nO_m(OCH_3)_p$ (n=2–4, m=1–11, p=0–6) are observed. Typical mass spectra under different source conditions are shown in Figure C.1. In particular, smaller fragments are obtained by increasing the high voltage applied on the source needle. The higher voltage increases the kinetic energy of the ions and therefore the strength of the collisions with curtain gas molecules (see Section 2.1.2). Note that the ion formation processes in the two cluster sources (laser vaporization source and electrospray source) are radically different: while in laser vaporization clusters are grown from atomic building blocks, in electrospray ionization clusters are the result of collision induced fragmentation of a larger species.
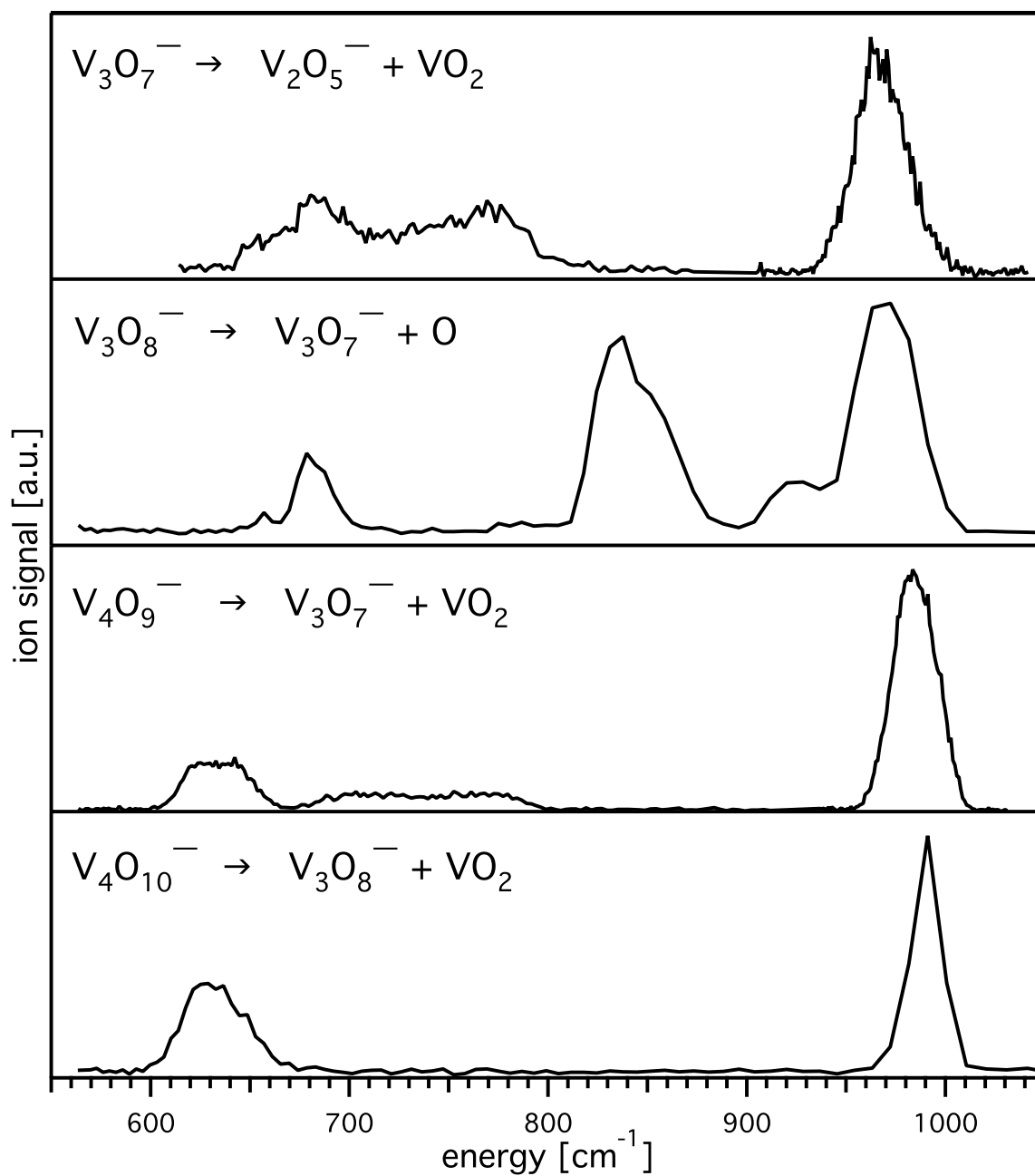
The IR-PD spectra of $V_3O_7^-$, $V_3O_8^-$, $V_4O_9^-$, and $V_4O_{10}^-$ produced by electrospray ionization are shown in Figure C.2. Upon photodissociation of $V_3O_7^-$ only $V_2O_5^-$ is observed as a photofragment (VO_2 loss). The strongest absorption band is found at 962 cm^{-1}, with a full width at half maximum of $\sim$30 cm^{-1}. Two other broad
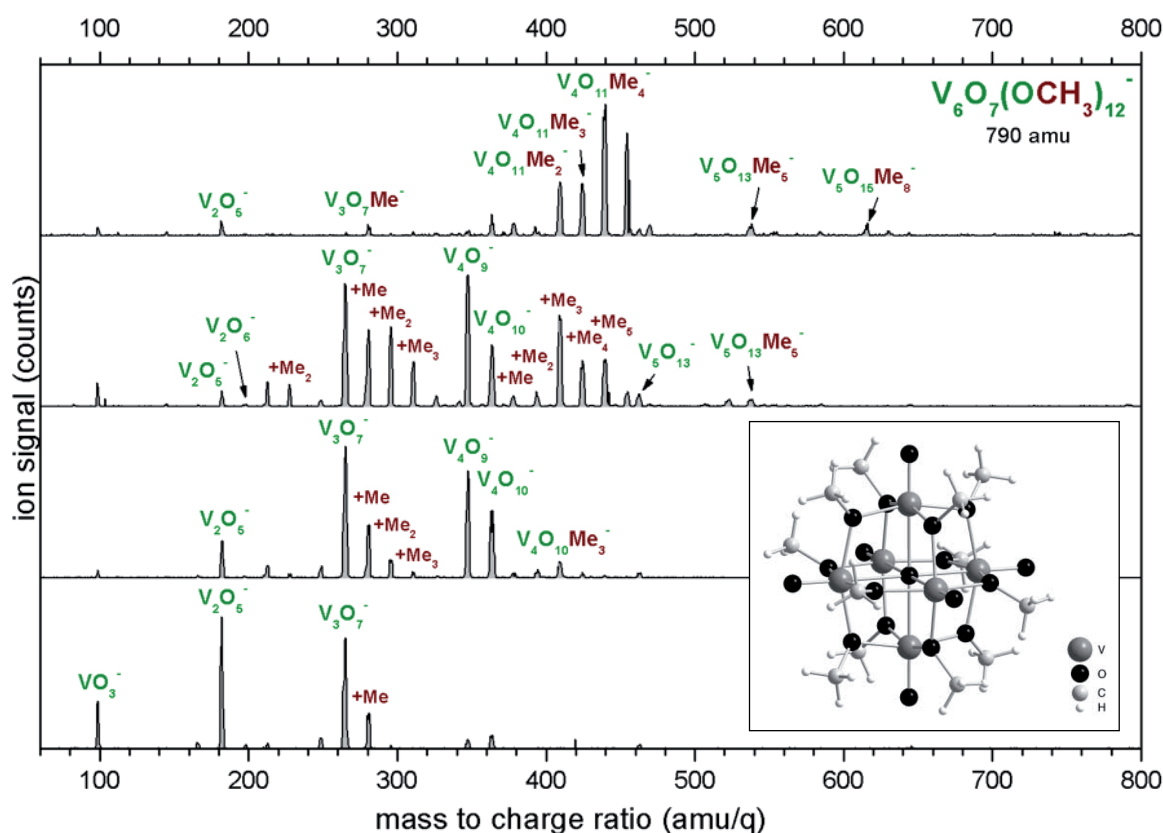
Figure C.1: Mass spectra obtained by electro-spraying a milli-molar solution of $V_6O_7(OCH_3)_{12}$ in methanol at a flow rate of ~ 2 μL/min. The high voltage applied on the source needle is progressively increased from top to bottom, producing smaller and smaller fragments of the $V_6O_7(OCH_3)_{12}$ precursor. The structure of the $V_6O_7(OCH_3)_{12}$ complex is shown in the insertion [298].

absorptions are observed with maxima at 769 and 684 cm^{-1}. The band found at 962 cm^{-1} is assigned to the vanadyl stretch, and the band at 684 cm^{-1} to the modes of the V$-$O$-$V bridges. The 769 cm^{-1} band remains unassigned. The only observed photofragment of $V_4O_9^-$ is $V_3O_7^-$ (VO$_2$ loss). The IR-PD spectrum of $V_4O_9^-$ is dominated by an intense band with maximum at 984 cm^{-1}. A second, broader feature appears at about 634 cm^{-1} and two weaker features centered at 715 and 780 cm^{-1}, respectively, are observed in-between. The intense band is assigned to the vanadyl stretch and the feature at 634 cm^{-1} coincides with the position expected for the modes of the bridging oxygen atoms, V$-$O$-$V. The assignment of the two weaker features remains unclear.

The IR-PD spectra of $V_3O_8^-$ and $V_4O_{10}^-$ produced by electrospray can be compared with those of the cluster with the same composition produced by laser vapor-

Figure C.2: IR-PD spectra of $V_3O_7^-$, $V_3O_8^-$, $V_4O_9^-$, and $V_4O_{10}^-$ produced by electrospray from a solution of $V_6O_7(OCH_3)_{12}$ in methanol.

ization. In Figure C.3 the spectra of these clusters produced with the two techniques are shown. Both for $V_3O_8^-$ and $V_4O_{10}^-$, IR-PD of the ions produced with the two different cluster sources gives identical spectra, as far as band positions are concerned
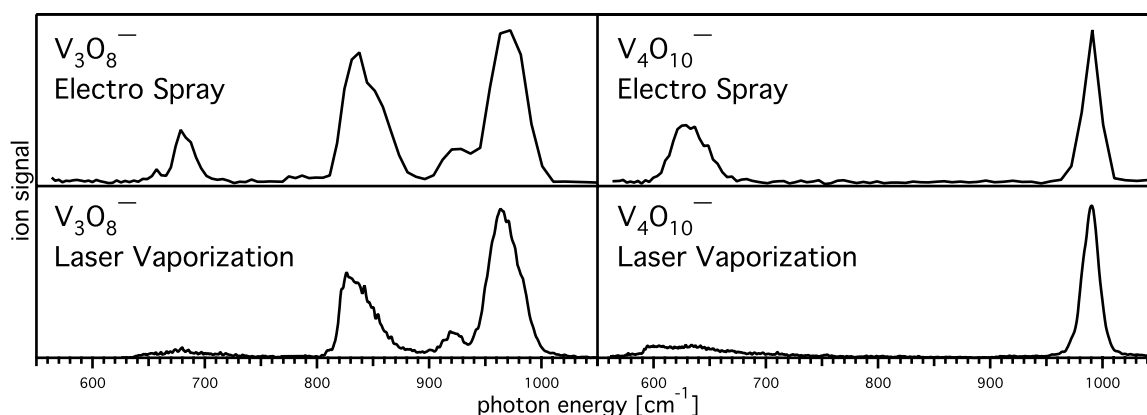
Figure C.3: IR-PD spectra of $V_3O_8^-$ and $V_4O_{10}^-$ produced by electrospray from a solution of $V_6O_7(OCH_3)_{12}$ in methanol (top) and produced by laser vaporization (bottom) (see also Chapter 3).

(see Chapter 3). Differences in relative intensities are found in the region below 750 cm^{-1}. They are most likely due to different laser powers in the low-energy region. Specifically, the ZnSe setup is used in the experiments with laser vaporization source, while the KRS-5 setup is used in the experiments with the electrospray source (see Section 2.2). The transmission efficiency of the ZnSe setup progressively drops with decreasing photon energy starting from 750 cm^{-1}. Therefore, both for $V_3O_8^-$ and for $V_4O_{10}^-$, the measured spectra must correspond to the same isomer. It has to be noted, however, that clusters are "adiabatically" cooled by many collisions with He buffer gas in the ion trap. This substantially reduces the possibility of finding kinetically-trapped metastable isomers.

The IR-PD spectra of $V_4O_9(OCH_3)^-$ and $V_4O_8(OCH_3)_2^-$ are shown in Figure C.4. The IR-PD spectrum of $V_4O_9(OCH_3)^-$ is measured monitoring the $V_4O_{10}^-$ photofragment (CH$_3$ loss). In addition to the vanadyl stretch at 999 cm^{-1}, the IR-PD spectrum shows a prominent peak at 1074 cm^{-1} with a smaller satellite at about 1130 cm^{-1}. In the region of the V$-$O$-$V bridging modes, a broad signal centered at 624 cm^{-1} is observed. The C$-$O stretch of free methanol lies at 1027 cm^{-1} in the gas phase and is found at about 1020 cm^{-1} in solution [295]. For methoxy surface-species on vanadia, slightly higher wavenumbers of about 1065 cm^{-1} have been reported [299, 300], whereas the bridging methoxy ligands of $V_6O_7(OCH_3)_{12}$ appear at 1031 cm^{-1} [298]. Therefore, the intense band observed at 1074 cm^{-1} is assigned to the C$-$O stretch and the weaker one at 1130 cm^{-1} to a CH$_2$ deformation mode.

The IR-PD spectrum of $V_4O_8(OCH_3)_2^-$ is generally similar to that of the monomethoxo cluster. It is obtained by monitoring the the $V_4O_{10}^-$ photofragment ((CH$_3$)$_2$ loss). Prominent features appear at 610, 997, and 1065 cm^{-1}, which are accordingly assigned to V$-$O$-$V bridging, vanadyl stretch, and C$-$O stretch modes, respectively.
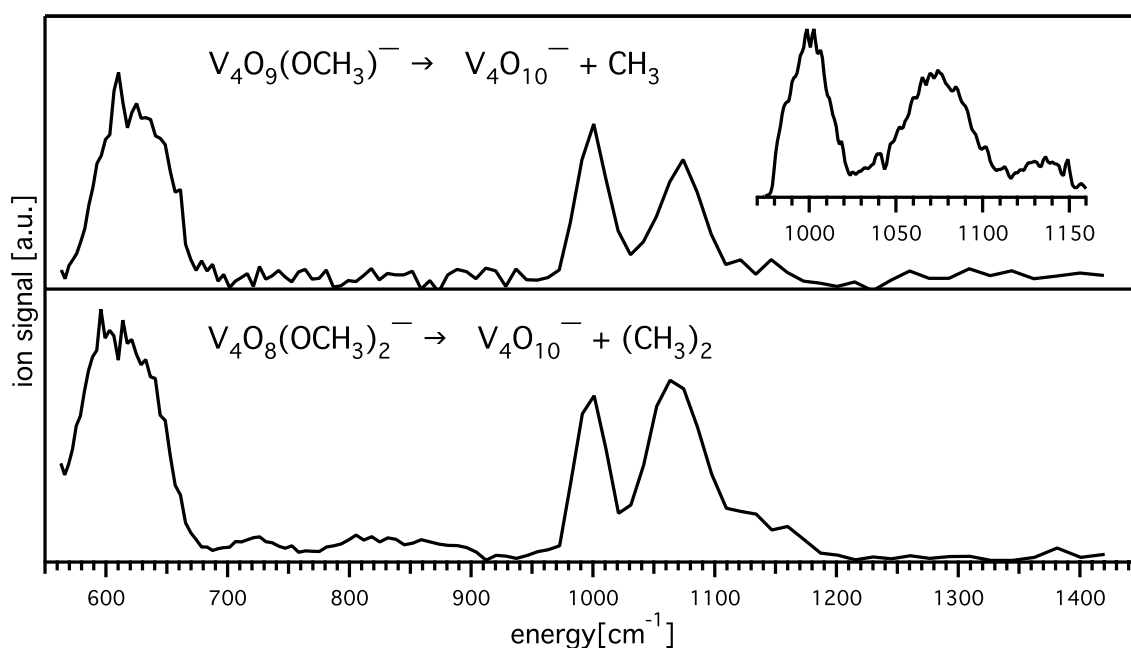
Figure C.4: IR-PD spectra of $V_4O_9(OCH_3)^-$ and $V_4O_8(OCH_3)_2^-$ produced by electrospray.

The major difference in the comparison of the $V_4O_9(OCH_3)^-$ and $V_4O_8(OCH_3)_2^-$ spectra is associated with the increased intensity of the C—O band relative to the other bands, which is consistent with the larger number of C—O oscillators at the expense of free vanadyl groups in the dimethoxo cluster. In comparison to the pure oxide clusters $V_4O_9^-$ and $V_4O_{10}^-$ (Figure C.2 bottom), clusters containing methoxo ligands show a much weaker intensity of the vanadyl band than would be expected from the mere consideration of the number of vanadyl moieties replaced by methoxo ligands. Again, weak features are observed between 700 and 900 cm^{-1}, which may be due to combination bands.

Even without computed IR spectra, some important structural conclusions can be drawn from the experiments. At first, the observation of the C—O bands in Figure C.4 indicates the presence of intact methoxy groups in the CH_3-containing clusters, and thus discounts the occurrence of a possible rearrangement to hydrido-metal species. Secondly, the relative increase of the C—O bands at the expense of the vanadyl modes indicates that the methoxo ligands replace some of the terminal oxo groups rather than acting as bridging ligands as in the case of the neutral $V_6O_7(OCH_3)_{12}$ [298]. The latter view is further supported by the slight blue shift of the C—O bands from 1031 cm^{-1} in $V_6O_7(OCH_3)_{12}$ to 1074 and 1065 cm^{-1} in $V_4O_9(OCH_3)^-$ and $V_4O_8(OCH_3)_2^-$, respectively. Hence, the IR spectra reveal structural details that could not have bee derived from the mass spectrometric fragmentation patterns alone [301].